J Electr Eng Technol.2017; 12(5): 1812-1820
http://doi.org/10.5370/JEET.2017.12.5.1812

ISSN(Print) 1975-0102
ISSN(Online) 2093-7423

Analysis of a Symmetric Active Cell Balancer with a Multi-winding Transformer

Seonwoo Jeon*, Myungchin Kim and Sungwoo Bae†**

Abstract – This paper analyzes a symmetric active cell balancer for a battery management system. The considered cell balancer uses a forward converter in which the circuit structure is symmetric. This cell-balancing method uses fewer switches and is simpler than the previously proposed active cell-balancing circuits. Active power switches of this cell-balancing circuit operate simultaneously with the same pulse width modulation signals. Therefore, this cell-balancing circuit requires less time to be balanced than a previous bidirectional-forward-converter-based cell balancer. This paper analyzes the operational principles and modes of this cell balancer with computer-based circuit simulation results as well as experimental results in which each unbalanced cell is equalized with this cell balancer. The maximum power transfer efficiency of the investigated cell balancer was 87.5% from the experimental results. In addition to the experimental and analytical results, this paper presents the performance of this symmetric active cell-balancing method.

Keywords: Active cell balancer, Forward converter, Multi-winding transformer, Series-connected battery cells

1. Introduction

To solve the energy crisis and lower CO_2 emissions in the industry, research on technology for novel energy applications have been actively conducted recently. Examples of such energy applications include photovoltaic (PV) system, energy storage system (ESS), plug-in hybrid vehicles (PHEVs), and electric vehicles (EVs) [1, 2]. In particular, electric vehicles use secondary cell battery systems to solve disadvantages of conventional internal-combustion-engine vehicles such as high dependence on fossil fuel and CO_2 emissions. By using high-voltage battery systems and electric traction systems, the energy conversion efficiency of electric vehicles could reach a higher level.

These applications require numerous battery cells that should be connected in series or in parallel. Unfortunately, to deliver power from a high-voltage battery pack to the electric traction system, an imbalanced cell problem cannot be avoided for series-connected battery strings. Such an imbalance between the battery cells is caused by the repetitive process of charging and discharging in high-voltage battery packs. Although the battery pack would be manufactured with multiple and identical battery cells, the impedance characteristics of each battery cell would be different from each other for practical reasons. While it is ideal for manufacturers to produce identical battery cells during serial production, various factors introduce differences in the battery cells (e.g., initial charge level). Examples of factors that introduce such variance include external temperature conditions, and different individual self-discharge rates [3, 4].

Furthermore, if an EV uses unequal secondary battery cells in the battery system without a cell balancing circuit, the highest-voltage-cell-connected battery string can be overcharged. The repetitive charging and discharging of imbalanced cells may lead to a decrease in the life span and rated capacity of individual cells [5]. In addition, if a high-voltage battery system does not have a cell-balancing device for series-connected battery strings, the highest-voltage cell can explode [6]. Thus, if a cell-equalizing device is used, overcharging and overdischarging can be solved before reaching a dangerous level. For these reasons, a cell-balancing device is essential to maintain proper safety conditions in the battery system.

When one of the cells in a battery pack has a problem, replacing that cell is the most straightforward solution. However, as cells are stored in the battery pack, replacement of a specific individual cell may be difficult and create a cost problem. Therefore, cell balancing is the proper solution for the problems stated above. Cell-balancing technologies such as passive cell balancing [7, 8] and active cell balancing [9-16] have been researched. A passive cell-balancing technology normally utilizes resistors to solve an overcharging problem due to higher energy cells in the battery pack [17]. Although this technology has the advantages of simple control and low production cost, it has lower efficiency than an active cell-balancing

† Corresponding Author: Dept. of Electrical Engineering, Hanyang University, Seoul, Republic of Korea (swbae@hanyang.ac.kr)
* Dept. of Electrical Engineering, Hanyang University, Seoul, Republic of Korea (01192112355@naver.com)
** School of Electrical Engineering, Chungbuk National University, Cheongju, Republic of Korea (mckim@chungcbuk.ac.kr)
Received: November 11, 2016; Accepted: January 3, 2017

technology because of heat dissipation at the resistor for protecting overcharged cells [18].

An active cell-balancing technology utilizes inductors, capacitors, and power electronic switches such as MOSFETs and IGBTs to balance cells by mutual transfer between cells connected in series or in parallel [7, 17]. Although this technology has higher efficiency compared with approaches that adopt a passive cell-balancing technology, it requires more time to balance its cell energy. In addition, an active cell-balancing technology generally requires a complex control algorithm with additional power electronic components so that the size of its circuit tends to be bulkier than that of a passive cell-balancing technology [19].

This paper analyzes a cell balancer based on a forward DC-DC converter [20, 21]. The considered active cell-equalizing circuit has a multi-winding transformer which transfers cell energy from higher-energy cells to lower-energy cells. Each cell is connected in series to the primary side of the transformer. As illustrated in Fig. 1, an active cell-balancing circuit with a previously proposed bidirectional forward converter [22] requires two active switches for each cell to balance each battery cell. Compared with such an approach, the cell-balancing circuit analyzed in this paper requires only one active switch for each cell, while the cell balancing time is also shorter than that of a cell-balancing circuit with a bidirectional forward converter [22]. While the operation principles and partial simulation results of the considered circuit have been discussed in [21], this paper expands the scope of discussion by providing more detailed analysis, performance characterization, and experimental verification results. Through such expansion, a more comprehensive analysis on the forward DC-DC converter based cell-balancing circuit has been established. The remainder of this paper is organized as follows: Section 2 explains the operational principles and circuit topologies of an active cell-balancing interface based on a forward converter in accordance with the on/off switch action. Section 3 describes computer-based simulation results to analyze the operation of the cell-balancing circuit. In Section 4, experimental results are presented along with the discussion on characteristics of the considered cell-balancing method. Section 5 concludes this paper with a summary.

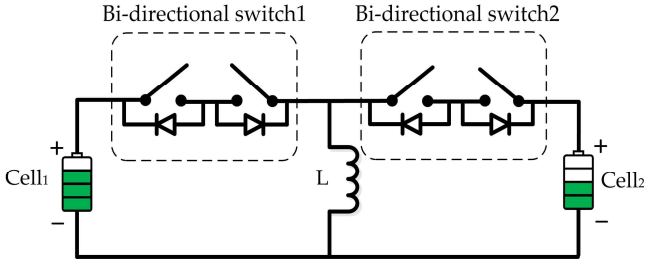

Fig. 1. Previous bidirectional cell balancer [22]

2. Structure and Operational Analysis of a Symmetric Cell Balancer

This section analyzes an active cell balancer based on a forward converter for series-connected battery strings. Then, the operational principles with mode analyses are introduced.

2.1 Active cell balancer based on a forward converter using a multi-winding transformer

Fig. 2 shows an active cell balancer with a forward converter for an analysis of its operational principles [21]. The considered cell balancer consists of N number of cells, N number of active switches that are connected to each cell, a diode, and a multi-winding transformer (T_m). While the active switches are used to connect each cell to the primary side of the transformer, the diode is installed between the secondary side of the transformer and the battery pack. In this active cell balancer, the turn ratio of the transformer is set as 1 (N_1/N_2) to transfer the energy of the unbalanced cell at the same rate. Moreover, all active switches ($S_1 \sim S_N$) installed between each cell and the primary side of the transformer are operated with the same pulse-width-modulation (PWM) signals. Therefore, the considered cell balancer enables direct energy transfer through the

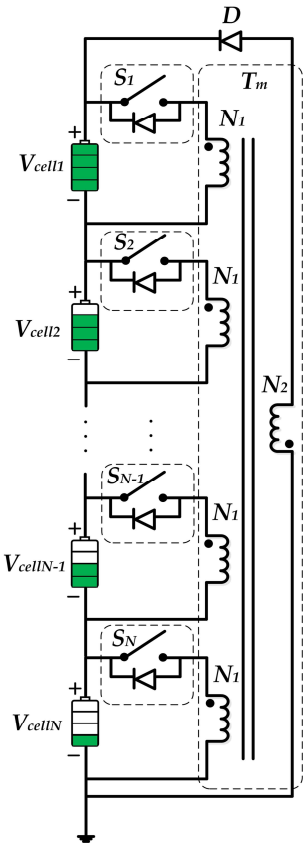

Fig. 2. Configuration of the considered active cell balancer using a multi-winding transformer [21]

transformer from the cells that have higher energy to the cells that have lower energy.

2.2 Operational principles with mode analyses

As stated above, the considered cell balancing interface is operated with the simultaneous conduction of active switches located at the primary side. By the simultaneous conduction of active switches, higher-energy cells transfer energy to lower-energy cells directly with the multi-winding transformer. The higher-energy cell has a higher open-circuit-voltage (OCV) value than other cells. Accordingly, the state-of-charge (SOC) level of the higher energy cell is relatively larger than that of others, the lower-energy cells. The conduction states of all active switches occur at the same time because all active switches operate according to the identical PWM signal with the same duty ratio.

Fig. 3 shows a cell-balancing circuit with three cells to investigate the operational principles and conduct an analysis on each operation mode. Because of the straightforwardness of this circuit operational analysis, the series-connected cells of Fig. 3 were assumed with the following conditions: the voltages of the three cells have the following relationship as

$$V_{cell1} < V_{cell2} < V_{cell3} \quad (1)$$

$$V_{cell2} = \frac{V_{Total}}{3} \quad (2)$$

$$V_{Total} = V_{cell1} + V_{cell2} + V_{cell3} \quad (3)$$

where V_{cell1}, V_{cell2}, and V_{cell3} are the voltage levels of $Cell_1$, $Cell_2$, and $Cell_3$, respectively, and V_{Total} is the sum of all three cell voltages. That is, the voltage of $Cell_3$ is the highest and the voltage of $Cell_1$ is the lowest.

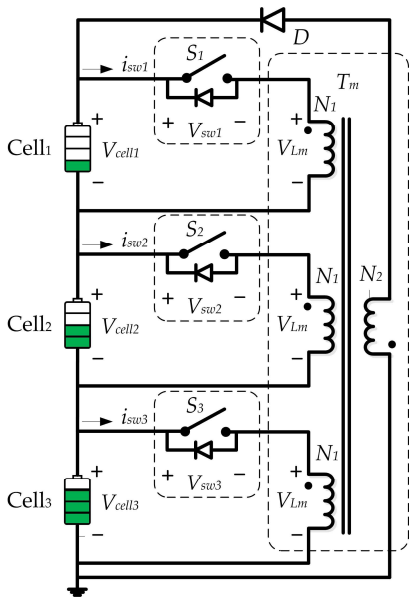

Fig. 3. Cell balancer for a 3-cell case [21]

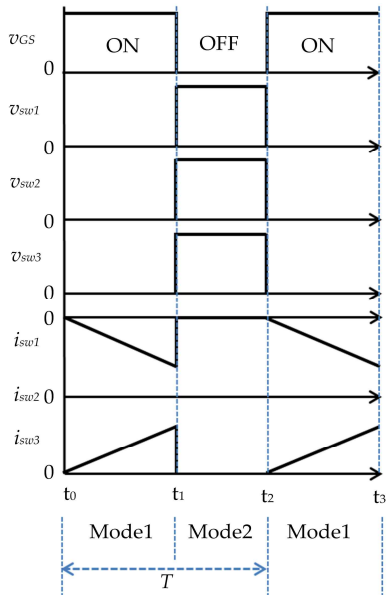

Fig. 4. Theoretical waveforms of the cell balancer

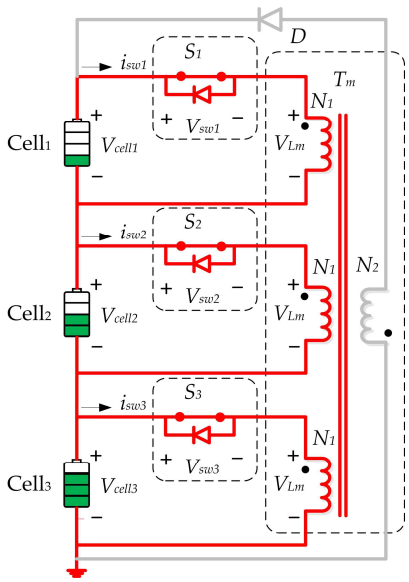

Fig. 5. Operation mode 1 of the cell balancer [21]

Fig. 4 shows theoretical waveforms of active switch currents and voltages with the same PWM signals. In accordance with the above conditions, operation of the cell-balancing circuit is divided into a conduction state of switches (i.e., Mode 1) and an open state of switches (i.e., Mode 2) during one switching period.

Mode 1 ($t_0 - t_1$): Fig. 5 shows the switch conduction mode with three cells. Using active conducting switches connected to the three cells at t_0, the voltages of the active switches become zero. Since the three active switches share the same PWM signal and duty ratio, the voltages of the active switches become zero at the same time. During this conduction period, the energy of the highest-voltage cell (i.e., $Cell_3$) is transferred to the lowest-voltage cell (i.e.,

$Cell_1$) through the multi-winding transformer (T_m) that is connected to the switches.

In order to analyze this conduction period, this cell-balancing circuit with three cells is transformed into the equivalent circuit as shown in Fig. 6. Fig. 6 describes a Laplace transform circuit for the three-cell case. Based on Fig. 6, each switch current for cell balancing in the conduction mode can be obtained as follows:

$$i_{sw3,peak}(t) = \frac{-V_{cell1} - V_{cell2} + 2V_{cell3}}{3R_{ds(on)}} e^{-\frac{t}{R_{ds(on)}C}} \quad (4)$$

$$i_{sw1,peak}(t) = \frac{2V_{cell1} - V_{cell2} - V_{cell3}}{3R_{ds(on)}} e^{-\frac{t}{R_{ds(on)}C}} \quad (5)$$

$$i_{sw2,peak}(t) = \frac{-V_{cell1} + 2V_{cell2} - V_{cell3}}{3R_{ds(on)}} e^{-\frac{t}{R_{ds(on)}C}} = 0A \quad (6)$$

where t is an instant during the conduction period. As shown in equations (4), (5), and (6), the peak switch currents (i.e., $i_{sw1,\,peak}(t)$, $i_{sw2,\,peak}(t)$, and $i_{sw3,\,peak}(t)$) can be expressed by the voltage values of the battery cells (i.e., V_{Cell1}, V_{Cell2}, and V_{Cell3}). During the conduction period, as switch currents depend on the active switch on-resistance, such a resistance value (i.e., $R_{ds(on)}$) needs to be considered in the circuit design stage for a high efficiency.

As shown in Fig. 4, the switch current of the highest-voltage cell (i.e., $i_{sw3,\,peak}(t)$) is positive, which denotes that it discharges energy to the lowest voltage cell (i.e., $Cell_1$). Meanwhile, the switch current of the lowest-voltage cell (i.e., $i_{sw1,\,peak}(t)$) has a negative value, which means that $Cell_1$ is charged for balancing by the highest-voltage cell (i.e., $Cell_3$). The switch current connected to $Cell_2$ (i.e., $i_{sw2,\,peak}(t)$) remains at zero because $Cell_2$ has the average voltage of the three cells at the initial condition.

Each switch current has a slope because of the leakage inductance (i.e., L_{lkg}) and mutual inductance (i.e., L_m) of the multi-winding transformer as shown in Fig. 4. The switch current increases or decreases with a constant slope. Therefore, both the leakage inductance and the mutual inductance value should be considered for design and operational analysis of the considered balancing circuit. In the switch conduction mode, each switch current can be calculated using equations (7)-(9). Therefore, when all components are ideal, $i_{sw1}(t)$ and $i_{sw2}(t)$ become

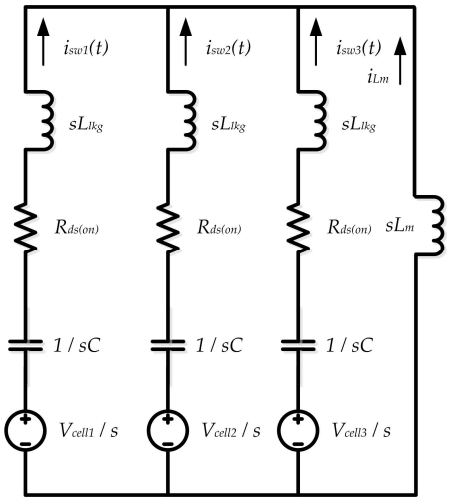

Fig. 6. Laplace transform circuit for the Mode 1 case

symmetrical. Cell energy transmission occurs because of only voltage difference between $Cell_1$ and $Cell_3$.

$$i_{sw3}(t) = \frac{-V_{cell1} - V_{cell2} + 2V_{cell3}}{L_{lkg}} e^{-\frac{(t-t_0)}{R_{ds(on)}C}} \quad (7)$$

$$i_{sw1}(t) = \frac{2V_{cell1} - V_{cell2} - V_{cell3}}{L_{lkg}} e^{-\frac{(t-t_0)}{R_{ds(on)}C}} \quad (8)$$

$$i_{sw2}(t) = \frac{-V_{cell1} + 2V_{cell2} - V_{cell3}}{L_{lkg}} e^{-\frac{(t-t_0)}{R_{ds(on)}C}} \quad (9)$$

Fig. 7 depicts the equivalent circuit for N cells to analyze the operation in the conduction mode. The equivalent circuit model consists of capacitors with initial voltages, the on-resistances of active switches (i.e., $R_{ds(on)}$), and the leakage inductances (L_{lkg}) of the multi-winding transformer. With the equivalent circuit, each switch peak current is derived by the differences between cells as follows:

As shown in Eq. (10), all cell currents in the battery string are symmetric for energy transmission between each other.

Mode 2 ($t_1 - t_2$): Fig. 8 shows the open-switch state mode with three cells. In this mode, the mutual inductance voltage (v_{Lm}) is controlled to reset; therefore, v_{Lm} is reset to zero by the secondary winding of the transformer and diode. During this operation mode, the charging-

$$i_{sw,peak}(t) = \begin{bmatrix} i_{sw_1}(t) \\ i_{sw_2}(t) \\ i_{sw_3}(t) \\ \vdots \\ i_{sw_k}(t) \\ \vdots \\ i_{sw_N}(t) \end{bmatrix} = \begin{bmatrix} N-1 & -1 & -1 & -1 & -1 & \cdots & -1 \\ -1 & N-1 & -1 & -1 & -1 & \cdots & -1 \\ -1 & -1 & N-1 & -1 & -1 & \cdots & -1 \\ \vdots & \vdots & -1 & N-1 & -1 & \vdots & \vdots \\ -1 & -1 & -1 & -1 & N-1 & -1 & -1 \\ \vdots & \vdots & \vdots & \vdots & -1 & \ddots & \vdots \\ -1 & -1 & -1 & -1 & -1 & \cdots & N-1 \end{bmatrix} \begin{bmatrix} V_1 \\ V_2 \\ V_3 \\ \vdots \\ V_k \\ \vdots \\ V_N \end{bmatrix} \frac{e^{-t/R_{ds(on)}C}}{NR_{ds(on)}} \quad (10)$$

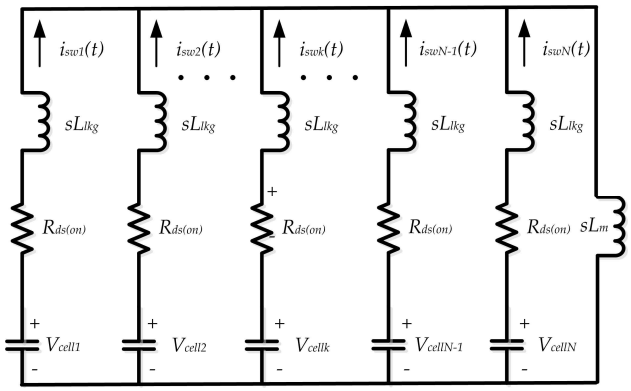

Fig. 7. Laplace transform circuit for the mode 1 of an *N*-cell case

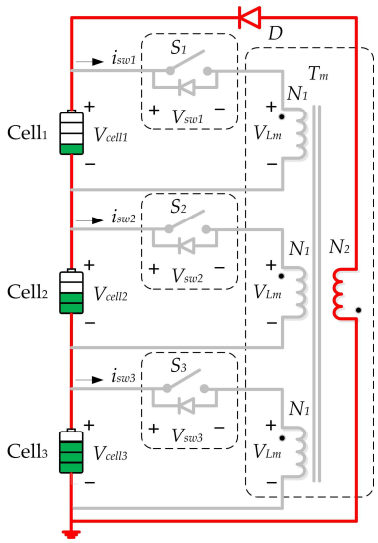

Fig. 8. Operation mode 2 of the cell balancer [21]

discharging process between cells is stopped. However, the switch current connected to $Cell_2$ (i.e., i_{sw2}) constantly remains at zero because $Cell_2$ is assumed to have the average voltage of the three cells by the initial conditions. In this mode, three active switches are conducted again at t_2 with the same PWM signal at the same time. Because of the conduction, the voltages of the active switches become zero, and the highest-voltage cell ($Cell_3$) transfers energy through the transformer to $Cell_1$ (i.e., the lowest-voltage cell). However, the switch current connected to $Cell_2$ (i.e., i_{sw2}) constantly remains at zero because of the initial conditions.

3. Simulation Analysis Results

This section describes computer-based circuit simulation analysis results in the considered cell balancer. For simplicity, all active switches including those of the multi-winding transformer and other components are assumed to be ideal. Table 1 lists the parameters used in this cell-balancing circuit simulation analysis. Under the initial conditions listed in Table 1, the voltage difference (i.e., ΔV) between the highest-voltage cell (i.e., $Cell_4$) and the lowest-voltage cell (i.e., $Cell_1$) was reduced from 0.3 V to 10 mV during a balancing time of 6 ms, as shown in Fig. 9.

As shown in Fig. 10, the switch currents of higher-voltage cells i_{sw1} and i_{sw2} have negative values which mean that $Cell_1$ and $Cell_2$ are charged for cell balancing by higher-voltage cells (i.e., $Cell_3$ and $Cell_4$). In addition, the switch currents of lower-voltage cells (i.e., i_{sw3} and i_{sw4})

Table 1. Parameters used in the cell balancer for simulation studies

Parameter name	Value	Unit
C	40	mF
initial V_{cell1}	3.5	V
initial V_{cell2}	3.6	V
initial V_{cell3}	3.7	V
initial V_{cell4}	3.8	V
D	0.475	N/A
L_m	100	mH
N_1/N_2	1	N/A
Switching Frequency	125	kHz

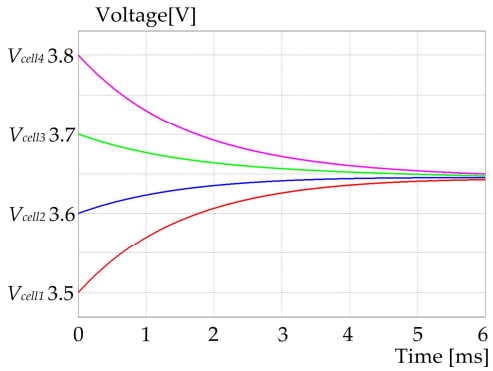

Fig. 9. Simulation result of a four-cell case

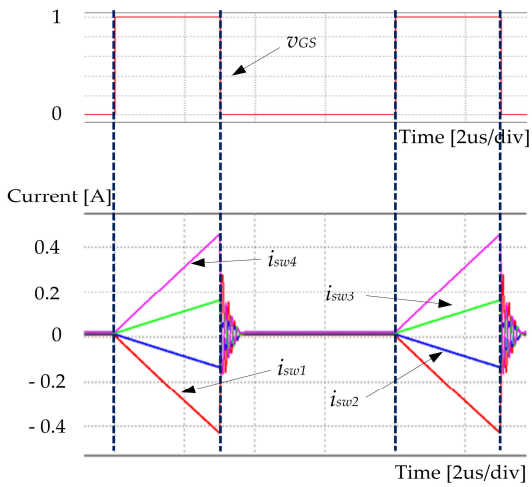

Fig. 10. Simulation result of four-cell case switching currents with the corresponding gate signal

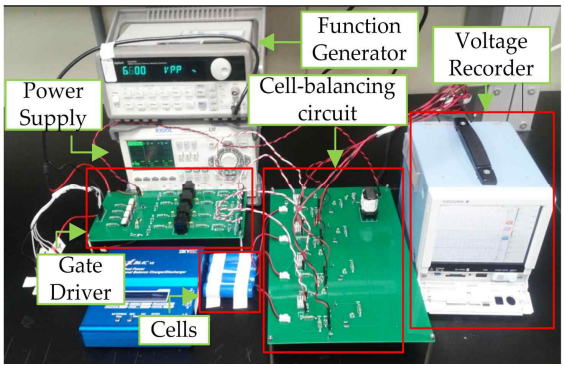

Fig. 11. Prototype of the cell-balancing circuit and experimental equipment

have positive values. Such a positive value represents that $Cell_3$ and $Cell_4$ are discharged for balancing. In Fig. 10, all cell currents (i_{sw1}~i_{sw4}) in the battery string are symmetric for energy transmission. As the voltage difference between the cells increases, the charging and discharging current values also increase. In other words, the balancing speed is fast when the voltage difference between the cells is large; however, as the voltage differences between cells decreases, the cell-balancing speed also decreases.

4. Experimental Results and Discussions

To verify the cell-balancing operation, a prototype circuit was fabricated and an experiment was performed with a two-cell Li-ion battery string. The circuit includes a cell-balancing circuit and a switch gate driver circuit to provide PWM signals, as shown in Fig. 11. The gate driver circuit of active switches includes opto-couplers, gate driver integrated circuits, and a transformer. This cell-balancing circuit can transfer unbalanced cell energy to other cells for the series-connected two-cell Li-ion battery string with the transformer. In addition, this cell-balancing interface is designed so that all series-connected cells to be equalized simultaneously.

The cell-balancing circuit was used in a two-cell battery string of an Li-ion battery pack (V_{cell1} = 3.68 V, V_{cell2} = 3.45 V, $Q_{cell1,\ 2}$ = 2200 mAh). The detailed specifications of the multi-winding transformer for the cell-balancing circuit were as follows: L_m is 100 mH, N_1/N_2 is 1, and an EER2928 core is used. Before the cell balancing process began, the voltage difference between the higher-voltage cell (i.e., V_{cell1}) and the lower-voltage cell (i.e., V_{cell2}) was 230 mV. When balancing operation between cells was started, switch current I_{sw} and switch voltage V_{sw} were measured as shown in Fig. 12. The current of the higher-voltage cell (i.e., V_{cell1}) has a positive value which means that it discharges and transfers energy to $Cell_2$. The current of the lower-voltage cell (i.e., V_{cell2}) has a negative value which implies that it charges and receives energy from $Cell_1$, as shown in Fig. 12(b). After 72 min, the voltage

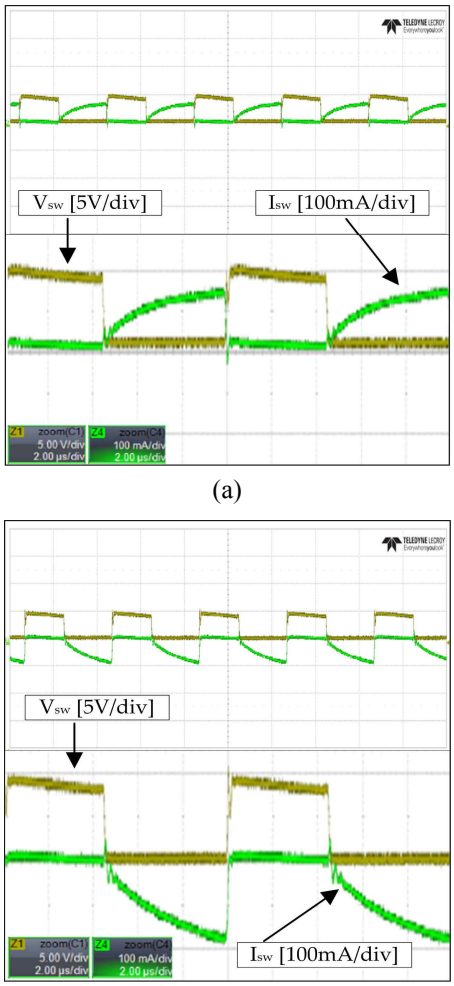

Fig. 12. Experimental waveforms of charging and discharging modes for a two-cell 2200-mAh Li-ion battery string. (a) Experimental waveforms of V_{sw} and I_{sw} in the discharging mode of $Cell_1$. (b) Experimental waveforms of V_{sw} and I_{sw} in the charging mode of $Cell_2$

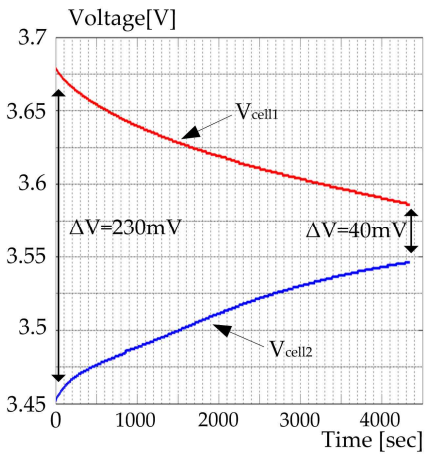

Fig. 13. Experimental waveforms of charging and discharging modes for a two-cell 2200-mAh Li-ion battery string

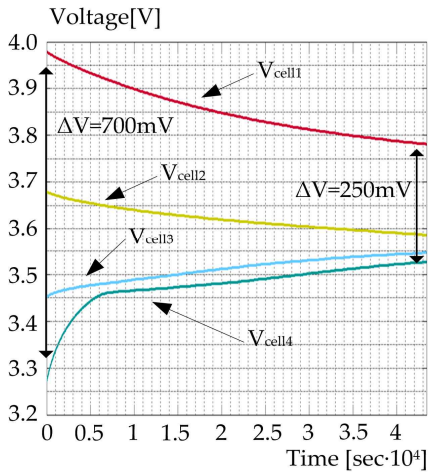

(a)

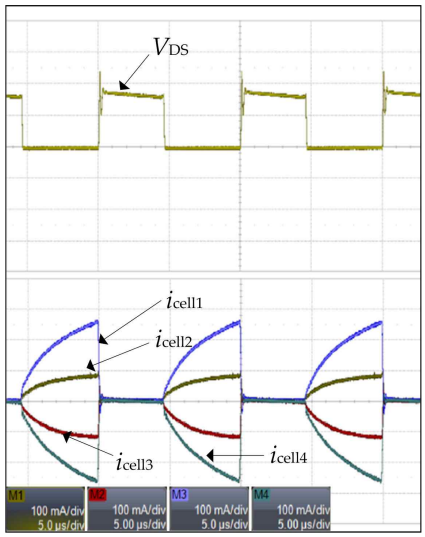

(b)

Fig. 14. Experimental waveforms for a four-cell 2200-mAh Li-ion battery string. (a) Cell balancing results. (b) Waveforms of V_{DS} and I_{sw} for the four-cell configuration

difference between V_{cell1} and V_{cell2} decreases to 40 mV, as shown in Fig. 13.

Another balancing circuit experiment was also conducted on a four-cell 2200-mAh Li-ion battery string. The highest voltage of a cell (i.e., V_{cell1}) was 3.97 V, and the lowest voltage of a cell (i.e., V_{cell4}) was 3.27 V. The other cells ($Cell_2$ and $Cell_3$) had values between 3.97 V and 3.27 V. This cell-balancing circuit has specifications as follows: D is 0.475, L_m is 100 mH, N_1/N_2 is 1, and an EER2928 core is used. Fig. 14(a) shows that the voltage difference (ΔV = 700 mV) between cells decreased to 250 mV. The theoretical waveforms and experimental results can be compared with Figs. 10 and 14(b), which indicates the switch voltage (i.e., V_{sw}) and current (i.e., I_{sw}). These experimental results showed that the considered cell-

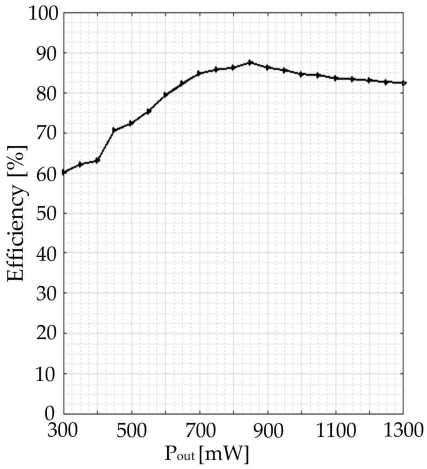

Fig. 15. Efficiency of the active cell balancer using a forward converter

balancing interface enables direct energy flow from the cells that have higher-energy to the cells that have lower-energy through the multi-winding transformer and active switches. As shown in Fig. 14, the larger the voltage difference between the cells is, the greater the charging and discharging current value are observed. Therefore, the balancing time can decrease if the voltage difference between the cells increases.

The efficiency of the considered cell-balancing approach was calculated from the input power data and the output power data. In the experiment results, the power for cell balancing transfers from the higher-voltage cells (i.e., $Cell_1$ and $Cell_2$) to the lower-voltage cells (i.e., $Cell_3$ and $Cell_4$), Hence, the input power can be obtained by the voltage and current data of the higher-voltage cells, while the output power can be calculated from the values of the lower-voltage cells. Fig. 15 shows the power transfer efficiency of the experimented cell balancer of which maximum value was 87.5%.

5. Conclusion

To ensure the safe performance and the maximum energy efficiency of rechargeable batteries such as lithium-ion, nickel-metal-hydrate, and nickel-cadmium in energy storage applications, a battery cell balancer is a necessary part of an energy management system. For a high-voltage battery pack connected with series multiple cells, the imbalanced cell problem cannot be avoided. In this study, an active cell balancer with a forward converter was considered. The cell balancing interface circuit used a multi-winding transformer for battery cell equalization by transferring the energy of higher-voltage cells to lower-voltage cell.

Since all switches are conducted with a constant duty ratio and the same PWM signal, the cell-balancing circuit

switches connected to each cell operate simultaneously to transfer cell energy for cell voltage equalization. Through this cell-balancing circuit, all cells are adjusted to the average cell voltage value of their series-connected battery string. Computer-based simulation results were provided to analyze the advantages and disadvantages of the considered cell balancing interface circuit. To analyze the real operation of this cell-balancing circuit, two-cell and four-cell Li-ion battery strings were used for experiments. The performance of the considered balancing circuit was verified with experiments, and the maximum power transfer efficiency of the cell-balancing circuit was 87.5%.

Acknowledgements

This research was supported by Basic Science Research Program through the National Research Foundation of Korea (NRF) funded by the Ministry of Science, ICT and Future Planning (NRF-2014R1A1A1036384).

This work was supported by the Korea Institute of Energy Technology Evaluation and Planning (KETEP) and the Ministry of Trade, Industry & Energy (MOTIE) of the Republic of Korea (No. 20161210200560).

References

[1] J. K. Na, K. S. Na, H. J. Lee, Y. S. Ko and C. Y. Won, "Power conversion system control method for hybrid ESS," *2014 IEEE Conference and Expo Transportation Electrification Asia-Pacific* (*ITEC Asia-Pacific*), pp. 1-5, Aug. 2014.

[2] J. Hongxin, F. Yang, Z. Yu and H. Weiguo, "Design of Hybrid Energy Storage Control System for Wind Farms Based on Flow Battery and Electric Double-Layer Capacitor," in *Proc. of Power and Energy Engineering Conference* (*APPEEC*), pp. 1-6, Mar. 2010.

[3] Y. Yang, M. Yao and Q. Wang, "Research on dynamic impedance characteristics of hybrid vehicle battery," in *Proc. of Industrial Technology (ICIT)*, *2014 IEEE International Conference on*, pp. 810-815. 2014.

[4] A. A. Hussein, "Experimental modeling and analysis of lithium-ion battery temperature dependence," *2015 IEEE Applied Power Electronics Conference and Exposition (APEC)*, pp. 1084-1088. 2015.

[5] G. Eason, B. Noble, and I. N. Sneddon, "On certain integrals of Lipschitz-Hankel type involving products of Bessel functions," *Phil. Trans. Roy. Soc. London*, vol. A247, pp. 529-551, Apr. 1955.

[6] A. Affanni, A. Bellini, G. Franceschini, P. Guglielmi and C. Tassoni, "Battery choice and management for new-generation electric vehicles," *IEEE Trans. Ind. Electron*., vol. 52, no. 5, pp. 1343-1349, Oct. 2005.

[7] H. S. Park, C. H. Kim, K. B. Park, G.W. Moon and J. H. Lee, "Design of a Charge Equalizer Based on Battery Modularization," *IEEE Trans. Veh. Technol*., vol. 58, no. 7, pp. 3216-3223, Sept. 2009.

[8] B. Lindemark "Individual cell voltage equalizers (ICE) for reliable battery performance," in *Proc. 13th Annu. Int. Telecommun. Energy Conf*., pp. 196 -201. Nov. 1991.

[9] N. H. Kutkut , H. L. N. Wiegman , D. M. Divan and D. W. Novotny, "Design considerations for charge equalization of an electric vehicle battery system," *IEEE Trans. Ind. Appl*., vol. 35, no. 1, pp. 28-35, Feb. 1999.

[10] M. Tang and T. Stuart, "Selective buck-boost equalizer for series battery packs," *IEEE Trans. Aerosp. Electron. Syst*., vol. 36, no. 1, pp. 201-211, Jan. 2000.

[11] Y. S. Lee and G. T. Cheng, "Quasi-resonant zero-current-switching bidirectional converter for battery equalization applications," *IEEE Trans. Power Electron*., vol. 21, no. 5, pp. 1213-1224, Sept. 2006.

[12] B. T. Kuhn, G. E. Pitel and P. T. Krein, "Electrical properties and equalization of lithium-ion cells in automotive applications," in *Proc. IEEE Vehicle Power Propuls. Conf.*, pp. 55-59, Sept. 2005.

[13] N. H. Kutkut, "Non-dissipative current diverter using a centralized multi-winding transformer," in *Proc. 28th IEEE Power Electron. Spec. Conf.*, pp. 648-654, Jun. 1997.

[14] S. T. Hung, D. C. Hopkins and C. R. Mosling, "Extension of battery life via charge equalization control," *IEEE Trans. Ind. Electron.*, vol. 40, no. 1, pp. 96-104, Feb. 1993.

[15] C. S. Moo, Y. C. Hsieh and I. S. Tsai, "Charge equalization for series-connected batteries," *IEEE Trans. Aerosp. Electron. Syst*., vol. 39, no. 2, pp. 704-710, April. 2003.

[16] N. H. Kutkut, "A modular non dissipative current diverter for EV battery charge equalization," in *Proc. 13th IEEE Annu. Appl. Power Electron. Conf. Expo.*, pp.686-690, Feb. 1998.

[17] J. W. Kim, J. W. Shin and J. I Ha, "Cell balancing control using adjusted filters in flyback converter with single switch," *2013 IEEE Energy Conversion Congress and Exposition* (*ECCE*), pp. 287-291, Sept. 2013.

[18] S. W. Moore and P. J. Schneider, "A review of cell equalization methods for lithium-ion and lithium polymer battery systems," in *Proc. SAE World Congr., Detroit, MI*, Doc. no. 2001-01-0959. Mar. 2001.

[19] Y. Ye, K. W. E. Cheng and Y.P.B Yeung, "Zero-Current Switching Switched-Capacitor Zero-Voltage-Gap Automatic Equalization System for Series Battery String," *IEEE Trans. Power Electron*., vol. 27, no. 7, pp. 3234-3242, Jul. 2012.

[20] M. Caspar, T. Eiler and S. Hohmann, "Comparison of Active Battery Balancing Systems," *2014 IEEE*

Vehicle Power and Propulsion Conference (VPPC), Coimbra, 2014, pp. 1-8.
[21] S. Jeon, J. J. Yun and S. Bae, "Active cell balancing circuit for series-connected battery cells," *2015 9th International Conference on Power Electronics and ECCE Asia (ICPE-ECCE Asia)*, Seoul, 2015, pp. 1182-1187.
[22] J. Yun, T. Yeo and J. Park, "High efficiency active cell balancing circuit with soft-switching technique for series-connected battery string," *Applied Power Electronics Conference and Exposition (APEC), 2013 Twenty-Eighth Annual IEEE*, Long Beach, CA, 2013, pp. 3301-3304.

Seonwoo Jeon received the B.S. and M.S. degrees from Yeungnam University, Gyeongsan, Korea all in electrical engineering, in 2014 and 2016. He is currently working toward the Ph.D. degree from Hanyang University, Seoul, Korea in the dept. of Electrical Engineering. His current research interests include a battery management system and a power conversion system for EVs/HEVs.

Myungchin Kim received the B.S. and M.S. degrees from Hanyang University, Seoul, Republic of Korea and Ph.D. degree from the University of Texas at Austin, USA, all in electrical engineering, in 2004, 2006, and 2015, respectively. From 2006 to 2017, he was with the Agency for Defense Development. He has been an Assistant Professor in the school of electrical engineering at Chungbuk National University in Korea since 2017. His research interests are in high voltage systems, novel power systems for emerging applications, and power electronics.

Sungwoo Bae received the B.S. degree from Hanyang University, Seoul, Korea, and the M.S.E. and Ph.D. degrees from the University of Texas at Austin, USA, all in electrical engineering, in 2006, 2009, and 2011, respectively. From 2012 to 2013, he was a senior research engineer with Power Center at Samsung Advanced Institute of Technology. From 2013 to 2017, he was with Yeungnam University. He has been an Assistant Professor in the dept. of electrical engineering at Hanyang University in Korea since 2017. In 2005, Dr. Bae was awarded the Grand Prize at the national electrical engineering design contest by the Minister of Commerce, Industry and Energy of the Republic of Korea.